Polish J. Chem., **78**, 1635–1654 (2004)

Multi-scan Voltammetric Determination of Carbohydrates at Noble Metal Microelectrodes Following Flow Injection and After Capillary Electrophoresis Separation*

by A. Basa, T. Krogulec and A.S. Baranski*****

Institute of Chemistry, University of Bialystok, 1 Hurtowa St., 15-399 Bialystok, Poland

(Received March 9th, 2004)

Two multi-scan techniques: cyclic voltammetry (CV) and fast Fourier transform square-wave voltammetry (FFT SWV) with Pt and Au microelectrodes were tested for the determination of five carbohydrates (lactose, sucrose, glucose, fructose and ribose) under FIA conditions. The best analytical results were obtained for the FFT SWV with a Pt microelectrode; in this case the detection limits were below 2×10^{-7} mol· dm^{-3} for all studied analytes. In addition, both methods were applied for end-capillary detection in capillary electrophoresis (CE) and tested during an analysis of a mixture of eight sugars. The advantages of scanning methods over constant potential (amperometric) detection methods are also discussed.

Key words: scanning voltammetry, square-wave voltammetry, electrochemical detection, flow injection analysis, capillary electrophoresis, carbohydrates

Electrochemical oxidation of carbohydrates, and in particular, glucose, has been intensively studied for many years. This attention is caused, among other things, by potentially practical applications of electrochemical glucose sensors and by a growing interest in biological fuel cells [1,2]. Many papers devoted to the investigation of glucose oxidation have been published (see for example [3]). Platinum and gold electrodes [4] have been the most widely investigated, although other metals such as Ni [5] and Cu [6] have been also examined as potentially better electrode materials.

It is generally accepted that a platinum surface can catalyze the electrochemical oxidation of glucose to gluconic acid [7]. The catalytic action of platinum is particularly significant in alkaline solutions. There are many papers showing that other carbohydrates, for instance D-xylose [8], exhibit similar behavior.

According to Johnson and LaCourse [9], the effectiveness of Pt and Au electrodes is largely due to the tendency of sugars to adsorb on their surface, where they readily undergo an electrochemical reaction. There is no doubt that adsorption of carbohydrates on a Pt surface plays an important role in their oxidation [10,11]; however, such suggestions regarding an Au electrode surface evoke some doubts. Larry and Johnson

* Dedicated to Prof. Dr. Z. Galus on the occasion of his 70th birthday.

** Corresponding author: krogulec@uwb.edu.pl

*** On sabbatical leave from Department of Chemistry, University of Saskatchewan at Saskatoon, Canada.

[12] propose a mechanism of glucose oxidation based on the assumption that glucose directly adsorbs on the gold electrode surface; however, others authors pointed out that there is no clear indication of glucose adsorption on gold [11] and that a gold oxide layer, electrochemically formed on the surface of gold, is a powerful and rather selective catalyst for the oxidation of glucose and other sugars [13]. Currently, most authors do not postulate a direct adsorption of carbohydrates on a gold surface. An extensive discussion of carbohydrate behavior on gold and platinum electrodes can be found in a recent review [14].

Noble metal electrodes, in particular Pt and Au, can be used in the electrochemical detection of many different kinds of analytes [4,15]. Unfortunately, the accumulation of oxidation products of organic compounds generally leads to electrode poisoning and a rapid decline of the detector response. As a remedy, anodic detection schemes typically consist of three potential steps (detection, desorption and conditioning), in order to maintain stable activity of Pt or Au electrodes. Detection based on such a scheme was first reported in 1981 by Hughes and Johnson [16] and it is called Pulsed Amperometric Detection (PAD). PAD, as well as Amperometric Detection at Constant Potential (ADCP), has been used for the detection of carbohydrates after separation by high-performance liquid chromatography (HPLC) or capillary electrophoresis (CE) [14,16,17]. Although PAD is still the most popular detection method used in analysis of sugars, it has significant drawbacks. First, the sensitivity of the detector declines with time as the electrode surface becomes contaminated (despite conditioning cycles). Second, if the electrode or mobile phase is changed, the values of the three potential steps and their duration must be optimized again. Third, the reproducibility of the method is often unsatisfactory.

It is therefore the aim of this work to investigate the possibility of using other electrochemical detection methods based on scanning voltammetric techniques in the detection of carbohydrates separated by capillary electrophoresis. These methods are especially designed for analytes, which adsorb on the electrode surface; the detection is carried out in a stripping mode after the accumulation of analytes on the electrode surface for 50 to 1000 ms. The stripping is performed under Cyclic Voltammetric (CV) or Fast Fourier Transform Square-Wave Voltammetric (FFT SWV) conditions. During the stripping step, the electrode is scanned in a desired range of potential and the electrode response is integrated over a certain potential interval. These detection methods were used for the determination of metal ions [18] and surface-active compounds [19] in the CV mode and for the determination of phenothiazines [20] and nonelectrochemically active analytes [21] in the FFT SWV mode. We believe that scanning techniques such as CV and FFT SWV are very valuable, not only because they are excellent detection tools, having all the advantages of PAD, but first of all, because these techniques enable studies of the nature of complex electrode processes in flowing solutions, exactly under the detection conditions.

EXPERIMENTAL

Reagents. All studied carbohydrates (D-raffinose, sucrose, α-lactose, D-galactose, D-glucose, D-mannose, D-fructose and D-ribose) were analytical grade and purchased from either Sigma (St. Louis, USA) or Fluka (Berlin, Germany). Mobile phases were prepared from carbonate-free sodium hydroxide solution for HPCE (Merck). All solutions were prepared in deionized water (KB-5522 DW from Cobrabid-AQUA, Warsaw, Poland) and were brought to the desired concentration by dilution with a mobile phase every day prior to use. Electrochemical measurements were carried out without removal of dissolved oxygen.

Electrodes. Working electrodes were made by sealing 10 μm (in radius) Pt and 12.5 μm (in radius) Au wires (Mennica Panstwowa, Warsaw, Poland) into Corning Kovar Sealing glass tubing #7052 (World Precision Instruments). A lead was made by connecting copper wire with micro-wires with the aid of silver epoxy. The capillary tubes were then cut perpendicular to their length to expose the wires. Next, the electrodes were polished with 1000- and 2000-grade carborundum paper and finally mirror-like polishing was accomplished using 3- and 0.3-μm aluminum oxide finishing films (TrueView Products Inc., USA).

The auxiliary electrode was made of a platinum wire, 0.5 mm in diameter. The reference electrode was Ag/Ag_2O in 0.1 mol $\cdot$ dm^{-3} NaOH. 0.1 mol $\cdot$ dm^{-3} NaOH was also used as a running buffer in flow injection and capillary electrophoresis experiments.

Apparatus and electrochemical cells. Measurements were carried out with a custom built electrochemical data acquisition system (EDAS). EDAS is based on a microcontroller (Microchip PIC18F452), which is interfaced with a computer *via* a serial link. Potential waveforms were generated by a 16-bit digital-to-analog converter (Linear LTC1655). The current was sampled by a 16-bit analog-to-digital converter (Texas-Instruments TLC4545) after passing through an anti-aliasing filter made of a clock-tunable 5th order Bessel low pass filter (Linear LTC1065). The maximum sampling rate was 120 kHz. The timing of all events was controlled by the microcontroller, with 100 ns accuracy.

Electrophoresis in a fused silica capillary (50 cm long with I.D. of 25 μm and O.D. of 375 μm) was performed in a plexiglass box equipped with an interlock system for operator safety. Separation voltage was provided by a high-voltage (0$\div$25 kV) power supply model no. 25A12-P4-F-M (UltraVolt, USA). The electrochemical detection cell placed at the cathodic end of the fused capillary was housed in a Faraday cage to reduce electrical environmental noise. The operation of all parts of the experimental setup was controlled by a computer. The code for the microcontroller was written in assembly language (with an assembler provided by Microchip) and the PC software (for data acquisition and processing) was written using Microsoft Visual C++, version 6.0 and Visual Basic, version 6.0. Admittance data were obtained by means of the Fast Fourier Transformation.

The diagrams of electrochemical cells used in flow injection and capillary electrophoresis experiments, as well as technical details of FIA and CE experiments, were described in our earlier paper [20]. All experiments were performed at room temperature at about 22°C.

Detection procedure. The potential waveform used in the FFT SWV is shown in Fig. 1. The acquisition of the detector response is carried out during the potential scan. In cyclic voltammetric experiments, the potential waveform is similar (except that scanning is performed in both directions, from initial potential to vertex and back to initial and there is no square-wave modulation superimposed). The scan rate in the CV experiments can be set between 1 mV $\cdot$ s^{-1} and 1000 V $\cdot$ s^{-1}. The scan rate in FFT SWV experiments depends on the square-wave frequency and on the potential range ($\upsilon = \Delta E \cdot f/128$, where: υ is the scan rate in V $\cdot$ s^{-1}, ΔE is the potential range in V and f is the frequency in Hz). The conditioning steps can be omitted, if the electrode is scanned in a sufficiently wide potential range, approaching O_2 and H_2 evolution potentials. The preconcentration time and preconcentration potential can be adjusted according to experimental requirements. A detailed description of the FFT SWV technique was provided earlier [20].

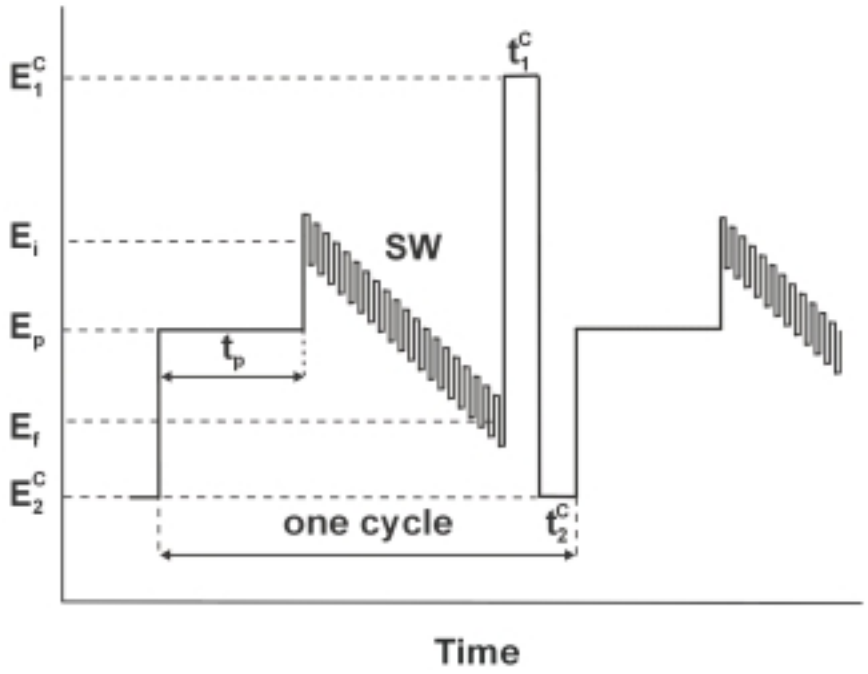

Figure 1. The potential waveform used in the FFT square-wave voltammetry. Each cycle starts at the preconcentration potential E_p applied for 50 to 2000 ms (t_p): then the electrode is polarized with a potential ramp from the initial (E_i) to the final (E_f) potential with a superimposed square wave modulation of a 50–200 mV amplitude and a 250–1500 Hz frequency. At the end of each cycle, the electrode is conditioned for t_1^c and t_2^c time periods at E_1^c and E_2^c potentials, respectively. The electrode response is sampled during the scan and the sampling frequency is at least 8 times higher than the square-wave frequency.

RESULTS AND DISCUSSION

The electrochemical behavior of sugars is commonly examined in strongly alkaline media such as 0.1 mol·dm^{-3} NaOH. This solution is also appropriate for the separation of sugars in capillary electrophoresis, because at high pH sugars form anions (pK_a is ranging from 11.94 to 12.51 [22] for examined sugars). It should be noted that the migration of dissociated sugars towards the anode in strongly alkaline solutions is always slower than the electroosmotic flow, moving in the opposite direction; consequently, sugars driven by the electroosmotic flow travel towards the cathodic end of the capillary.

CV experiments. In order to establish the best detection parameters for CE we carried out several preliminary CV and FFT SWV experiments. The examinations under the CV conditions were done at different scan rates (from 0.01 to 80 V·s^{-1}) in 0.1 mol·dm^{-3} NaOH solution containing various sugars at concentrations ranging from 5×10^{-7} (or less in some cases) to 0.1 mol·dm^{-3},with both Au and Pt microelectrodes.

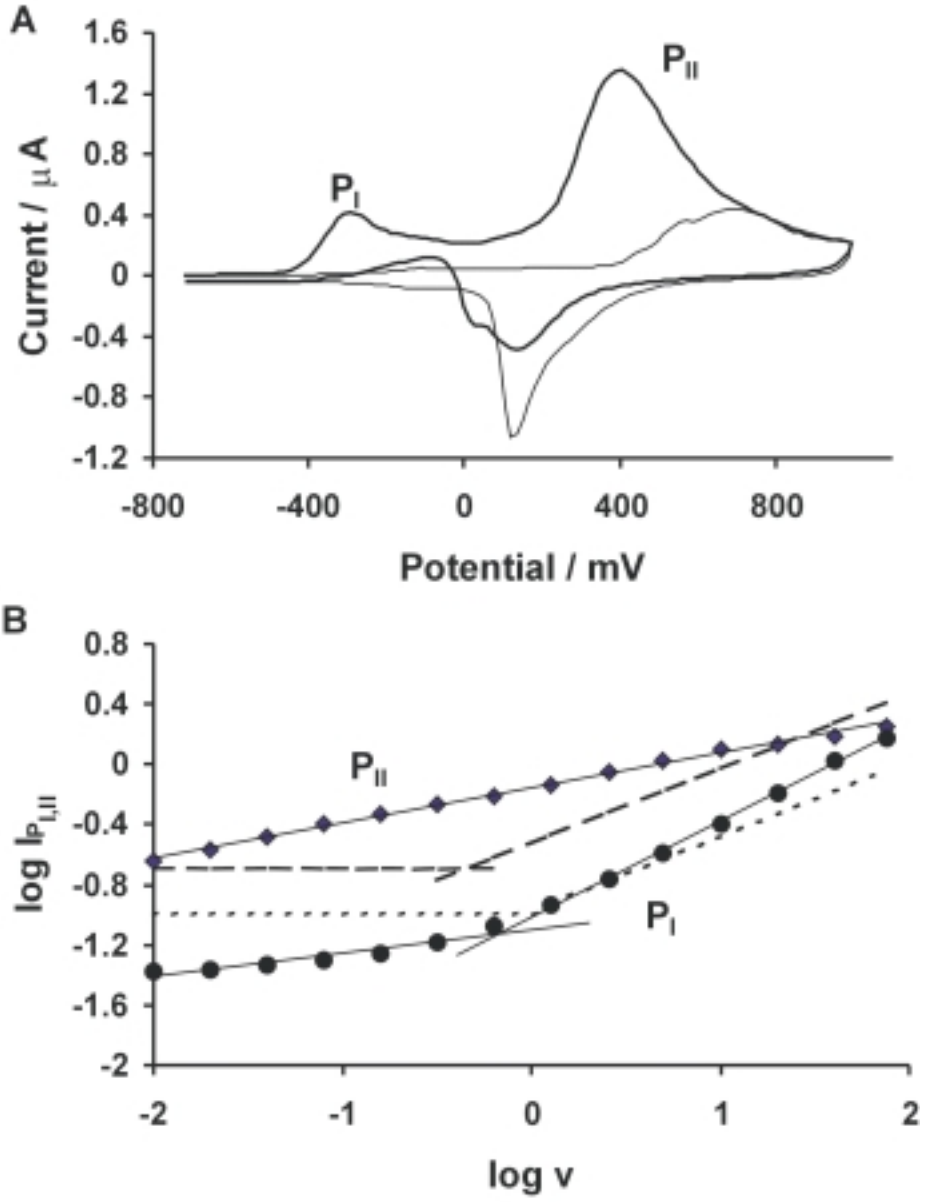

Figure 2. (A) CVs of an Au microelectrode at 10 $V \cdot s^{-1}$ obtained in a solution containing 3×10^{-2} $mol \cdot dm^{-3}$ glucose and 0.1 $mol \cdot dm^{-3}$ NaOH (thick line) or 0.1 $mol \cdot dm^{-3}$ NaOH (thin line). (B) Plots of log I_{PI} and log I_{PII} *vs.* log v for peak P_I (•) and peak P_{II} (◆) obtained with an Au microelectrode in 3×10^{-2} $mol \cdot dm^{-3}$ glucose and 0.1 $mol \cdot dm^{-3}$ NaOH. The dashed lines were calculated based on equations (1) and (2) for n = 1 (lower) and n = 2 (upper curve).

A CV response observed for a 3×10^{-2} mol·dm^{-3} solution of glucose in 0.1 mol·dm^{-3} NaOH is shown in Fig. 2A. Two peaks, P_I and P_{II}, are formed in the double layer region of the Au electrode during a scan from negative to positive potentials. The effect of the scan rate on the peak heights is presented in Fig. 2B. To make sure that observed changes are not caused by the aging of the electrode, the measurements were taken by changing the scan rate from small to large values and back from large to small, with practically the same results. At scan rates smaller than 0.2 V·s^{-1} peak P_I becomes very small and its height is practically independent of the scan rate. For example, in the case of glucose at scan rates smaller than 0.2 V·s^{-1}, the slope of $\partial \log I_{P_I}/\partial \log v$ for glucose is less than 0.1 (see Table 1). At higher scan rates ($v > 1$ V·s^{-1}) the slope of this dependence increases strongly to a value somewhat larger than 0.5. Peak P_{II} always increases with the scan rate, but more slowly than peak P_I ($\partial \log Ip_{II}/\partial \log v \approx 0.23$) and at a scan rate of about 80 V·s^{-1} the heights of both peaks become equal.

Table 1. Slopes of $\log I_p$ *vs.* $\log v$ plots for main voltammetric peaks caused by the oxidation of glucose on Au and Pt microelectrodes in 0.1 mol·dm^{-3} NaOH.

Electrode	Solution	Peak	Sweep rate range (V·s^{-1})	$\partial \log Ip/\partial \log v$
Au, $\phi = 25\,\mu$m	3×10^{-2} mol·dm^{-3} glucose + 0.1 mol·dm^{-3} NaOH	P_I	0.01÷0.20	0.10±0.01
		P_I	1÷80	0.64±0.01
		P_{II}	0.01÷80	0.23±0.01
Pt, $\phi = 20\,\mu$m	0.1 mol·dm^{-3} glucose + 0.1 mol·dm^{-3} NaOH	G_I	0.02÷0.5	1.63±0.06
		G_I	1÷80	0.48±0.02
		G_{II}	0.04÷80	0.54±0.02
		G_{III}	0.01÷0.4	0.53±0.02
		G_{III}	0.4÷20	0.11±0.02
	0.1 mol·dm^{-3} NaOH	H_I	0.02÷80	0.97±0.01
		O_I	0.1÷80	1.17±0.05
		O_{II}	0.02÷80	1.00±0.03

In linear potential scan voltammetry the peak current at a planar electrode is given by [23]:

$$I_p = 0.446 \frac{n^{3/2}F^{3/2}}{R^{1/2}T^{1/2}} AD_{Red}^{1/2} V^{1/2} c_{Red}^{0} \tag{1}$$

where: I_p is the peak current, c_{Red}^{0} is the concentration of the reactant, D_{Red} its diffusion coefficient, A the electrode surface area, V the scan rate, and n the number of electrons exchanged between one ion or molecule of a reactant and the electrode. F and R are Faraday and gas constants.

The same equation can be used to describe the peak current observed at a disk microelectrode at high scan rates. In this case, the peak current is proportional to the square root of the scan rate; however, at low scan rates, the maximum current at a disk microelectrode becomes independent of the scan rate and it is given by [23]:

$$I_m = 4nFc^0_{\mathrm{Re}d} D_{\mathrm{Re}d}\, r_0 \qquad (2)$$

where: r_0 is the radius of the electrode.

The dashed lines in Fig. 2B were calculated based on equations (1) and (2) for 3×10^{-2} mol·dm^{-3} glucose, assuming $D_{\mathrm{Re}d} = 7\times10^{-6}$ cm^2·s^{-1} and n = 1 (lower line) or n = 2 (upper line). The data obtained for peak P_I correlate well with the theoretical lines, which suggests that the process responsible for this peak may be controlled by diffusion.

Data presented in Fig. 2 do not show any evidence of adsorption of glucose on gold, but the process is obviously electrocatalytic (*i.e.* depends on the nature of the electrode material); therefore, that process must involve adsorption of the depolarizer (although the surface concentrations of glucose on gold may be very small).

Both peaks P_I and P_{II} are well developed at high scan rates, and integration of current over the whole oxidation potential range can be used to obtain a very good detection signal in flowing systems such as FIA, CE or HPLC. Some authors [16,24] express the opinion that integrated voltammetric detection (IVD) is too slow to monitor very narrow peaks of carbohydrates, and that constant potential amperometric detectors are preferable for CE [25]. This conclusion, however, arises from wrong assumptions regarding possible sweep rates. Integrated voltammetric detection with scan rates around 80 V·s^{-1} can be as fast as average constant potential amperometric detection, and it is well suited for CE detection, even in the case of very narrow analyte zones. It should be noted that peaks due to oxidation of glucose at a gold electrode are large only at large concentrations of glucose. At a concentration smaller than about 2×10^{-4} mol·dm^{-3}, the peak P_I disappears completely and in the region of peak P_{II}, only a small increase of current is observed. Nevertheless, the integration of current changes occurring at a scan rate of 2 V·s^{-1} in the potential region of P_{II}, allows us to determine glucose at a concentration of about 2×10^{-7} mol·dm^{-3}.

All other sugars studied in this work produce peak P_{II} that depends on the scan rate in a similar way to that described above. However, peak P_I does not appear for fructose and other carbohydrates that do not have aldehyde group –CHO. That has some practical analytical consequences, making it possible to determine glucose in the presence of fructose and other ketoses.

Figure 3A shows CV curves obtained with a Pt microelectrode in a 0.1 mol·dm^{-3} NaOH (thin line) and in a 0.1 mol·dm^{-3} NaOH containing 0.1 mol·dm^{-3} glucose (thick line). Such a large concentration of glucose in this supporting electrolyte was commonly used by others authors [3,11,26], but their studies were always done with Pt electrodes of standard (millimeter) size. There are three peaks corresponding to the oxidation of glucose. The first peak (G_I) coincides with hydrogen desorption peaks observed on Pt in NaOH (H_I and H_{II}) and the two other glucose oxidation peaks (G_{II} and G_{III}) coincide with platinum oxide formation peaks (O_I and O_{II}). The effect of the scan rate on the height of these peaks is shown in Fig. 3 B–D and in Table 1. Dashed lines in Fig. 3B show mass transport limits predicted by equations (1) and (2) for 0.1 mol·dm^{-3} glucose and for n = 1 (lower line) or n = 2 (upper line). All peaks observed

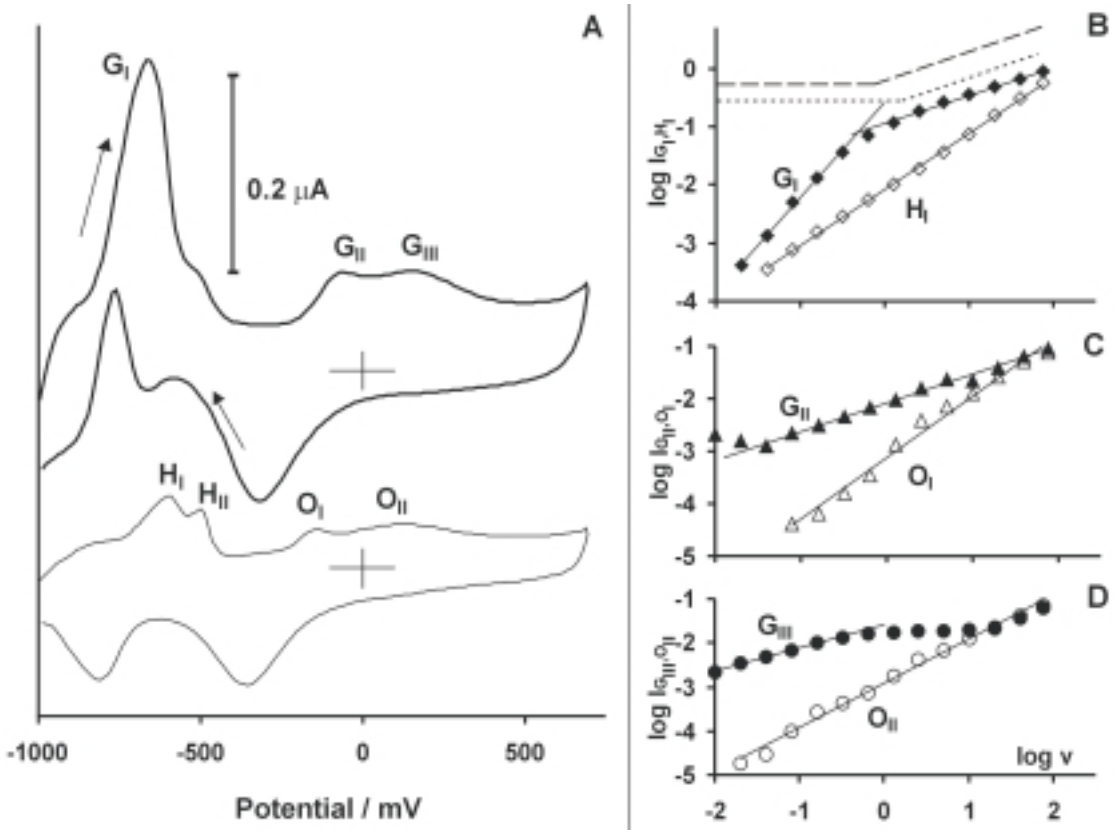

Figure 3. A: CVs of a Pt microelectrode at 10 $V \cdot s^{-1}$ obtained in a solution containing 0.1 $mol \cdot dm^{-3}$ glucose and 0.1 $mol \cdot dm^{-3}$ NaOH solution (thick line) or in 0.1 $mol \cdot dm^{-3}$ NaOH (thin line). B, C and D: Plots of logarithms of I_{GI}, I_{GII} and I_{GIII} *vs.* log *v* for peaks G_I (B), G_{II} (C) and G_{III} (D) obtained with a Pt microelectrode in 0.1 $mol \cdot dm^{-3}$ glucose and 0.1 $mol \cdot dm^{-3}$ NaOH (filled points ◆, ▲ and •) or in 0.1 $mol \cdot dm^{-3}$ NaOH alone (empty points ◇, Δ and O for peaks H_I, O_I and O_{II}). The dashed lines in B were calculated based on equations (1) and (2) for n = 1 (lower) and n = 2 (upper curve).

on Pt in pure NaOH exhibit slopes ∂ logI/∂ log v close to 1 as expected for adsorption/desorption processes. The heights of the glucose peaks were measured by subtracting the background current observed in 0.1 mol·dm^{-3} NaOH at corresponding potentials. At low scan rates, peak G_I increases very quickly with an increase of the scan rate; the slope ∂ logI_{G_I}/∂ log v is higher than 1.5. However, at scan rates higher than 1 V·s^{-1}, the slope (∂ logI_{G_I}/∂ log v) is close to 0.5. Also, peak G_{II} gives the slope close to 0.5 in the whole range of scan rates. A similar slope is also observed for peak $G_{III,}$ but only at scan rates lower than 0.4 V·s^{-1}; at higher scan rates this peak stops increasing.

Among these peaks, G_I is the highest and the integration of current in its potential range gives an excellent detection signal, unfortunately, only at high concentrations of glucose. Data in Fig. 3 B show that there is an optimum scan rate (around 0.3 to 0.6 V·s^{-1}) for which the ratio of the G_I current to the H_I current is the highest ($I_{G_I}/I_{H_I} \approx$ 20). Such a large ratio of both currents cannot be explained by simple oxidation of adsorbed glucose, since the surface concentration of adsorbed glucose cannot be larger than the surface concentration of adsorbed hydrogen.

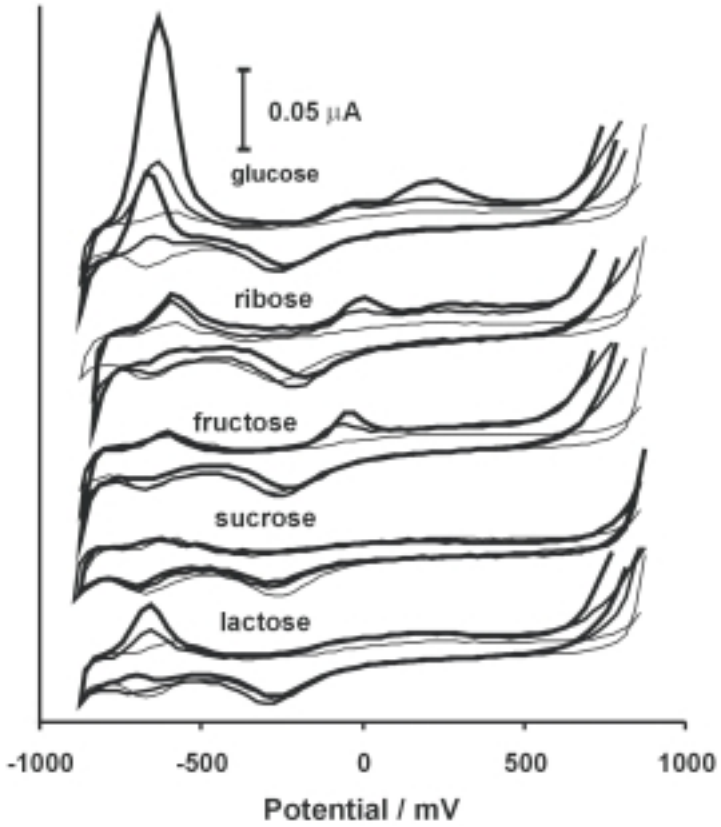

Figure 4. CVs for glucose, ribose, fructose, sucrose and lactose in 0.1 mol·dm^{-3} NaOH obtained with a Pt microelectrode at 1 V·s^{-1}. The thin lines were recorded in the absence of sugars, the thicker for a 0.01 mol dm^{-3} concentrations of sugars and the thickest – for 0.1 mol·dm^{-3}.

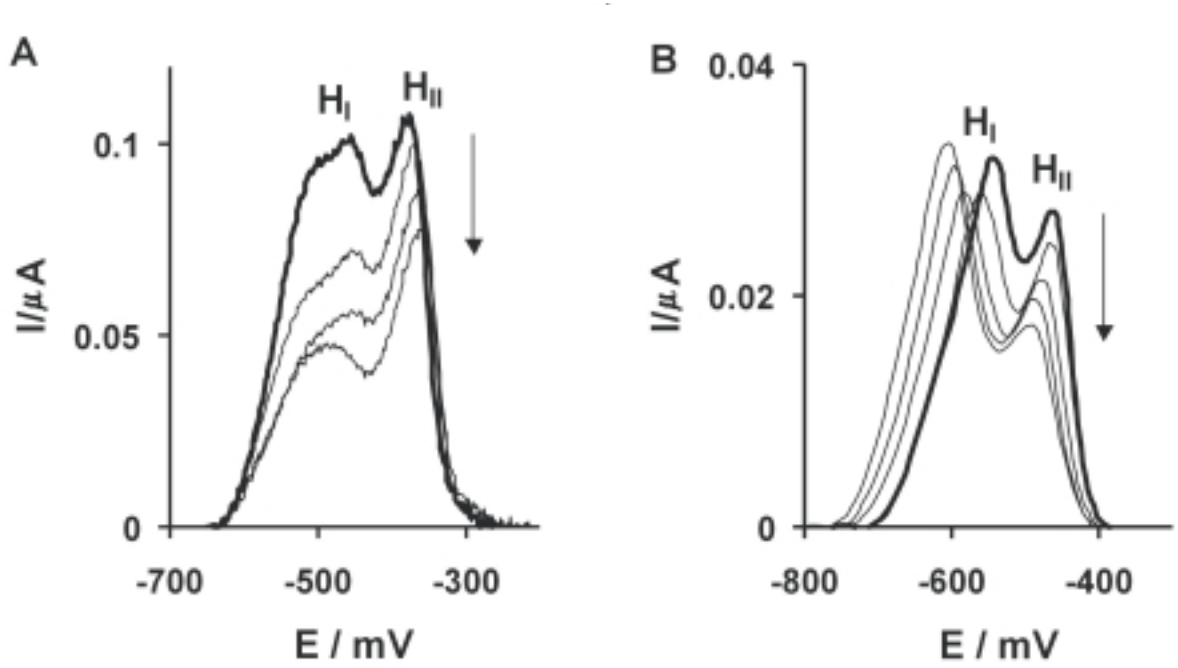

Figure 5. Changes in H_I and H_{II} peaks observed on CV curves at a Pt microelectrode during the injection of fructose (A) and lactose (B). Concentrations of fructose were 5×10^{-5}, 2×10^{-4} and 8×10^{-4} mol·dm^{-3} and lactose 5×10^{-5}, 2×10^{-4}, 6×10^{-4} and 2×10^{-3} mol·dm^{-3}. The scan rates were 16V·s^{-1} for fructose and 6 V·s^{-1} for lactose. Arrows indicate the increase of concentration. The thick lines are for 0.1 mol·dm^{-3} NaOH used as the supporting electrolyte.

We also studied the effect of scan rate on the oxidation of others sugars. The cyclic voltammetric curves recorded at 1 $V \cdot s^{-1}$ for two concentrations of each analyte (0.01 and 0.1 $mol \cdot dm^{-3}$) are shown in Fig. 4. It should be noted that sucrose gives no oxidation peaks and fructose does not produce a peak in the hydrogen adsorption region.

The first peak (equivalent to G_I) is not visible at all at low concentrations of all sugars (including glucose), instead a slight decrease of both hydrogen desorption peaks is observed. The effect of fructose (at concentrations ranging from 5×10^{-5} to 8×10^{-4} $mol \cdot dm^{-3}$) and lactose (at concentrations ranging from 5×10^{-5} to 2×10^{-3} $mol \cdot dm^{-3}$) on the hydrogen desorption peaks (H_I and H_{II}) is shown in Fig. 5. The thick lines represent the curves recorded in pure NaOH solution and the arrows show a trend caused by an increase in the analyte concentration. For sucrose and fructose, the maximum effect occurs at a concentration of about 1×10^{-3} $mol \cdot dm^{-3}$, further increase of the analyte concentration does not produce any change in the peak heights. For others sugars, when the hydrogen desorption peaks stop decreasing, an oxidation peak (equivalent to G_I in Fig. 3) starts to form on top of H_I; at that point, H_{II} also starts to increase. The initial decrease of the hydrogen desorption peaks is most likely caused by a competitive adsorption of sugars on Pt surface. If so, one could use this effect to determine adsorption isotherms for sugars on platinum. Such a study is now in progress and the results will be published separately. We have discovered that the integration of current change in the hydrogen adsorption region at a scan rate no larger than 2 $V \cdot s^{-1}$ produces the best detection signal for carbohydrates at platinum microelectrodes under CV conditions. In flow-injections experiments, we obtained linear calibration curves for concentrations of carbohydrates ranging from 6×10^{-7} to 5×10^{-5} $mol \cdot dm^{-3}$.

FFT SWV experiments. Initial FFT SWV experiments were carried out to search for the best value of the square-wave frequency and the amplitude. In this optimization procedure, the signal to noise ratio and reproducibility of the measurements under FIA and CE conditions were taken into account. It was concluded that the best results can be obtained by using a 500 Hz frequency and a 100 mV amplitude (peak to peak).

Fig. 6A shows the admittance measured at the Pt and Au microelectrodes during an injection of 1×10^{-4} $mol \cdot dm^{-3}$ lactose in 0.1 $mol \cdot dm^{-3}$ NaOH. Part B of this Figure shows the same data as part A but after the subtraction of the background admittance recorded in 0.1 $mol \cdot dm^{-3}$ NaOH. At a Pt electrode, lactose causes a large increase in the admittance, mainly in the hydrogen adsorption region, whereas, the admittance at an Au electrode decreases somewhat in the double layer region. Changes of the Au electrode admittance are about five times smaller than changes of the Pt electrode admittance, for the same concentration of lactose. In addition, changes at the Au electrode were observed only in the case of disaccharides such as lactose or sucrose; no measurable change was noted for monosaccharides. It seems very likely that disaccharides adsorb on gold in the double layer region and the observed decrease in admittance is due to a decrease in the electrode double layer capacitance. On the other hand, monosaccharides such as glucose may not significantly absorb on gold in that potential range.

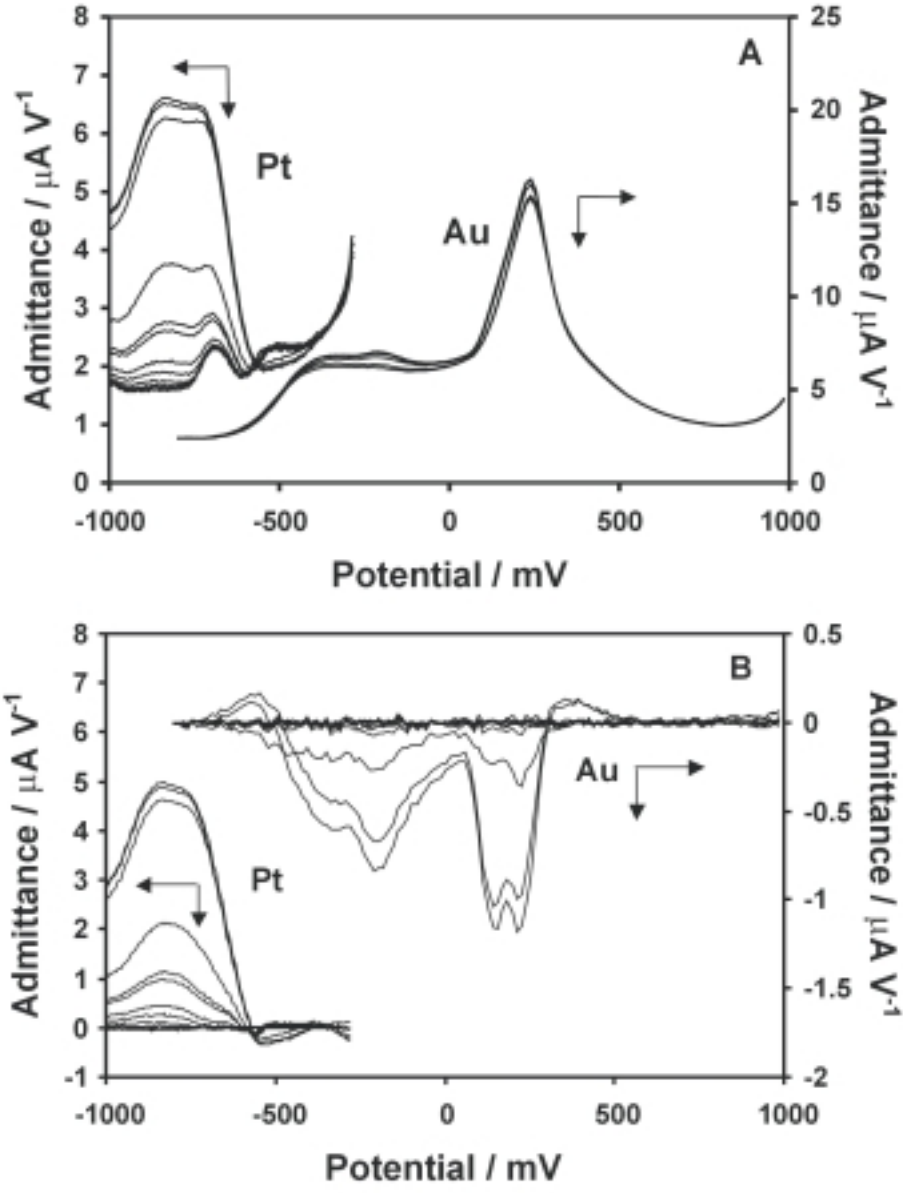

Figure 6. (A) Changes in the admittance-potential curves observed during the injection of 1×10^{-4} mol· dm^{-3} lactose in 0.1 mol·dm^{-3} NaOH. Measurements were carried out in a FFT SWV mode at gold (12.5μm in radius) and platinum (10μm) electrodes. The frequency was 500 Hz and the amplitude was 100 mV. (B) The same data as in (A) but after subtraction of the background admittance recorded in 0.1 mol·dm^{-3} NaOH.

On Pt electrodes the admittance in the hydrogen adsorption region increases in the presence of sugars. In order to understand that phenomenon we have to realize that sugars cannot completely suppress adsorption of hydrogen on Pt, because sugar molecules cannot block all sites on the Pt surface. This conclusion is in agreement with CV studies, which show that hydrogen desorption peaks become smaller in the presence of sugars, but they never completely disappear (Fig. 5). Hydrogen adsorption/desorption is a quasi-reversible process in NaOH at 500 Hz; the magnitude of the admittance associated with this process is relatively small, and as for all quasi-reversible processes, it is affected by the rate of the charge transfer. It is known from literature [27] that adsorption of some organic compounds can actually accelerate the charge transfer for the hydrogen adsorption/desorption processes. The observed increase of the Pt electrode admittance in the presence of sugars can be explained by such an effect. Importantly, sugars also accelerate the hydrogen evolution process. It should be noted that in the presence of sugars (at concentrations ranging from 4×10^{-7} to 5×10^{-5} mol $\cdot$ dm^{-3}) a significant change in current at the onset of the hydrogen evolution process is observed and that change contributes chiefly into the analytical signal generated under CV conditions. The practical consequence of this consideration is that a Pt microelectrode seems to be much better than an Au microelectrode for the determination of sugars under FFT SWV conditions.

To establish the best conditions for the determination of sugars at Pt microelectrodes under FFT SWV conditions, flow injection experiments were performed for each analyte. The effect of the initial potential, as well as the preelectrolysis and conditioning potentials on the magnitude of the signal for sucrose (A) and lactose (B), is shown in Fig. 7. Dependencies for the other sugars are similar. It should be noted that since the admittance (expressed in μA $\cdot$ V^{-1}) is integrated over a certain potential range (expressed in V), the units for the measured signal are in μA.

The presented results show that the best signals are obtained for initial and preelectrolysis potentials being situated in the double layer region. Each scan (from positive to negative potentials) should be preceded by a conditioning of a Pt microelectrode for a short time in the platinum oxide region. There is no need to condition the electrode at negative potentials. Preelectrolysis should be performed in a relatively narrow potential region (–400 to –600 mV for all examined sugars). In addition, the preelectrolysis time (in a range from 50 to 5000 ms) and conditioning time (in a range from 5 to 200 ms) were tested, and it was concluded that there is no benefit to increasing the conditioning time over 20 ms and the preelectrolysis time above 0.5 s.

Fig. 8 shows the three-dimensional view of FFT SWV curves recorded at a Pt microelectrode for six consecutive injections of 4×10^{-4} mol$\cdot$ dm^{-3} glucose in 0.1 mol$\cdot$dm^{-3} NaOH to NaOH solution, before (A) and after (B) subtraction of the background admittance. The change in the admittance caused by an injection of each examined sugar at 4×10^{-5} mol$\cdot$dm^{-3} concentration is shown in Fig. 9. The smallest change of the admittance is observed for fructose and the largest one for lactose (Fig. 9A). Clearly, processes responsible for these changes cannot be related to the process responsible for the voltammetric peak G_I shown in Fig. 4, although both processes occur in the same potential region (note that fructose do not produce peak G_I).

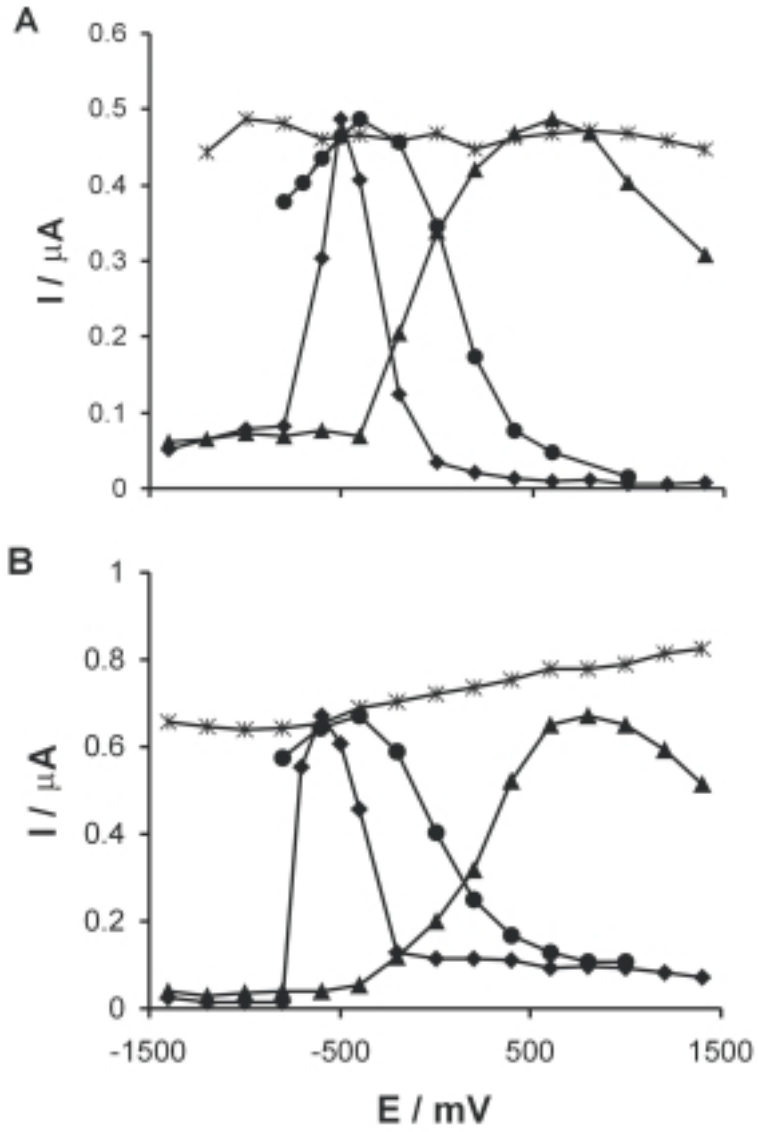

Figure 7. Effect of various experimental parameters on the detection signal of sucrose (A) and lactose (B), observed at a Pt microelectrode under FFT SWV conditions. Tested parameters: ◆ – preelectrolysis potential, • – initial potential (scan from positive to negative values), ▲ – first conditioning potential and ✳ – second conditioning potential. Detection signals were measured during a flow injection of 4×10^{-4} mol· dm^{-3} sucrose or lactose in 0.1 mol·dm^{-3} NaOH to 0.1 mol· dm^{-3} NaOH. Preconcentration time was equal to 1 s, both conditioning times were equal to 25 ms; when the effect of each parameter was tested, all others parameters were held at values which produce the maximum response.

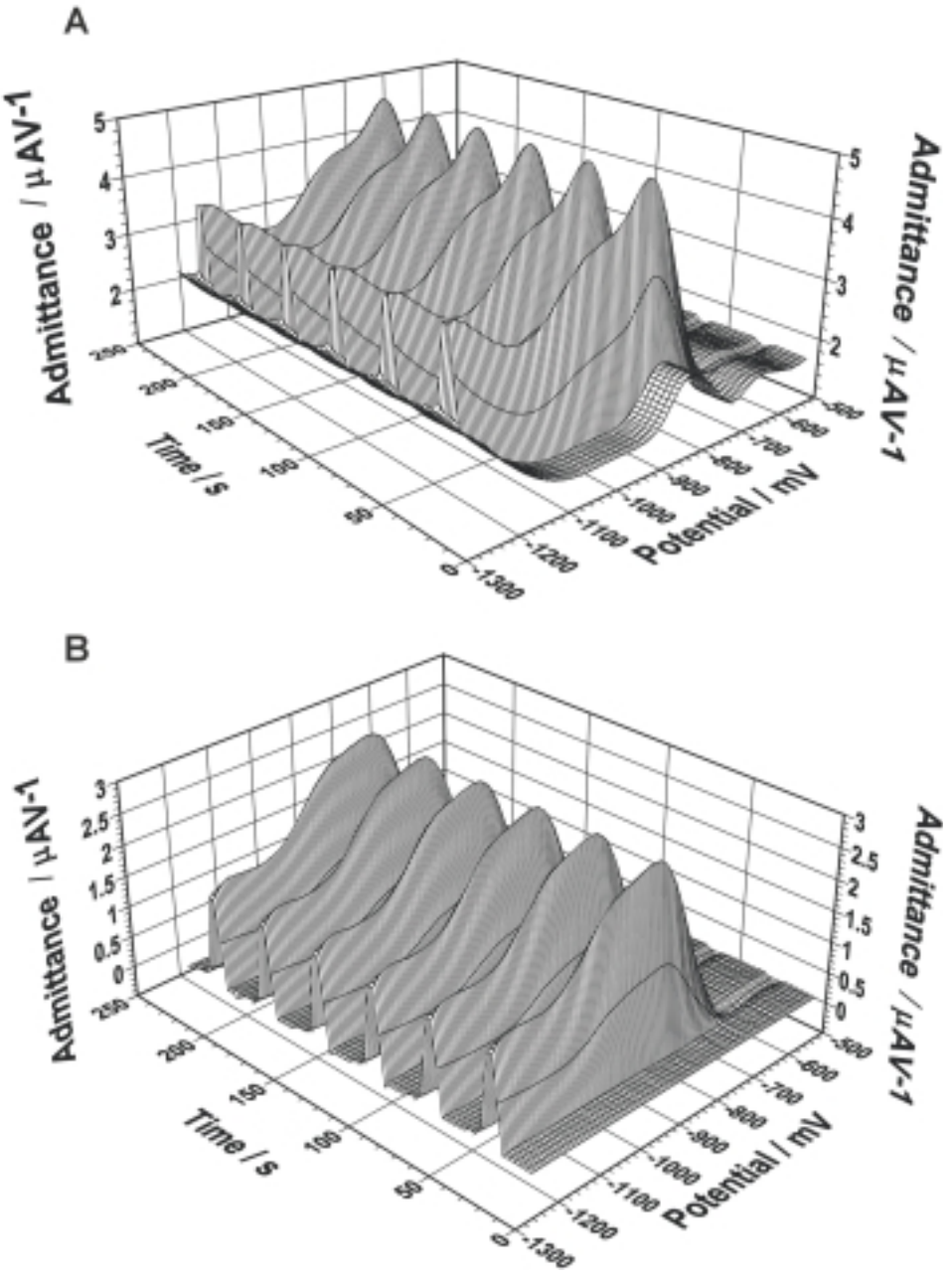

Figure 8. Three-dimensional FFT SWV admittance curves obtained with a Pt microelectrode during an injection of 4×10^{-5} mol·dm^{-3} glucose in 0.1 mol·dm^{-3} NaOH, before (A) and after (B) the subtraction of the background admittance. The experimental conditions were optimized following the procedure shown in Fig. 7.

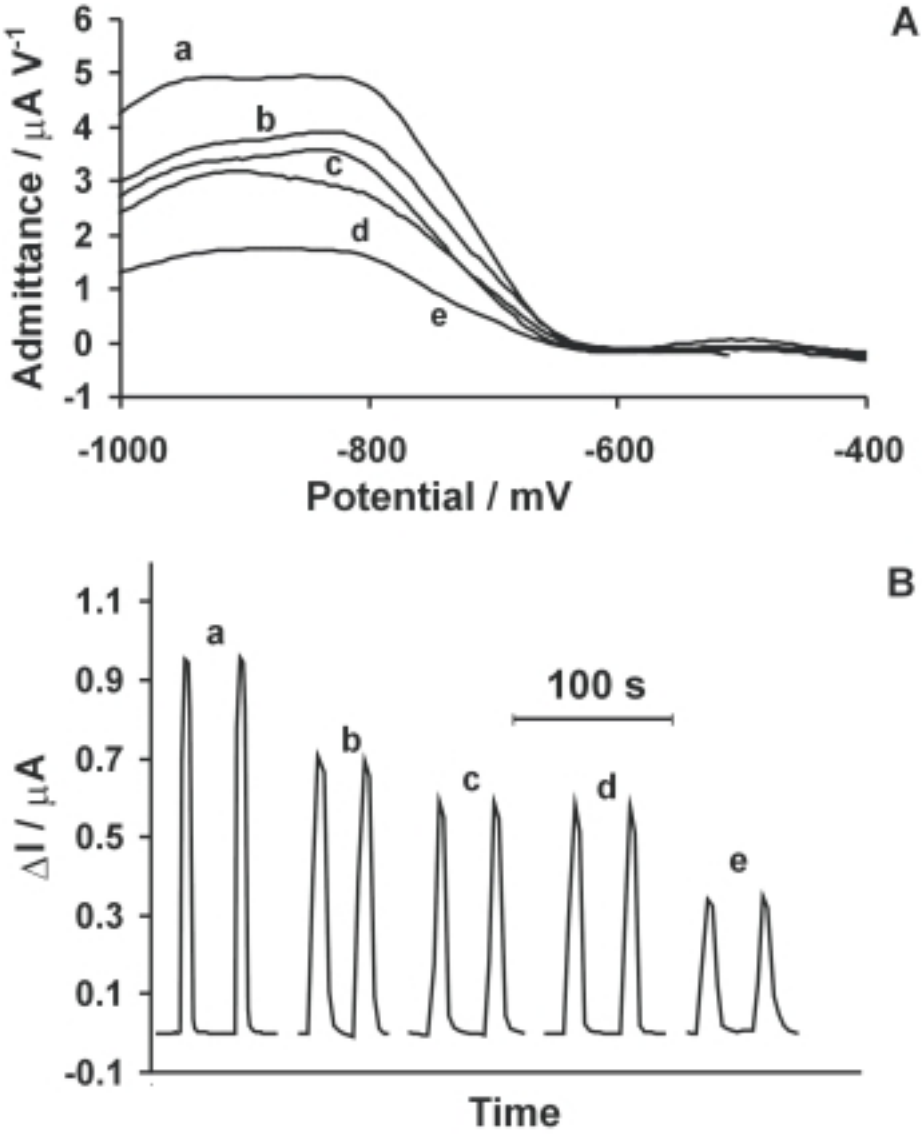

Figure 9. (A) Maximal changes of the electrode admittance after subtraction of the background admittance. (B) FIA peaks observed at a Pt microelectrode during injections of lactose (a), glucose (b), ribose (c), sucrose (d) and fructose (e) – all at 4×10^{-5} mol · dm^{-3}. The magnitude of the signal, ΔI in B, was obtained as a result of admittance integration over the whole potential range.

The changes in the Pt microelectrode admittance caused by the flow injection of various concentrations of glucose are shown in Fig. 10. Even for a concentration as small as 2×10^{-7} mol·dm^{-3}, admittance changes are significant enough to achieve the signal to noise ratio (S/N) of about 20. It shows that glucose can be detected at concentrations smaller than 1×10^{-7} mol·dm^{-3}. Others sugars at concentration 2×10^{-7} mol·dm^{-3} produce the S/N ratio ranging from about 20 for lactose to 8 for fructose. The calibration curves of all examined sugars were linear for concentrations ranging from 2×10^{-7} to 1×10^{-5} mol·dm^{-3}.

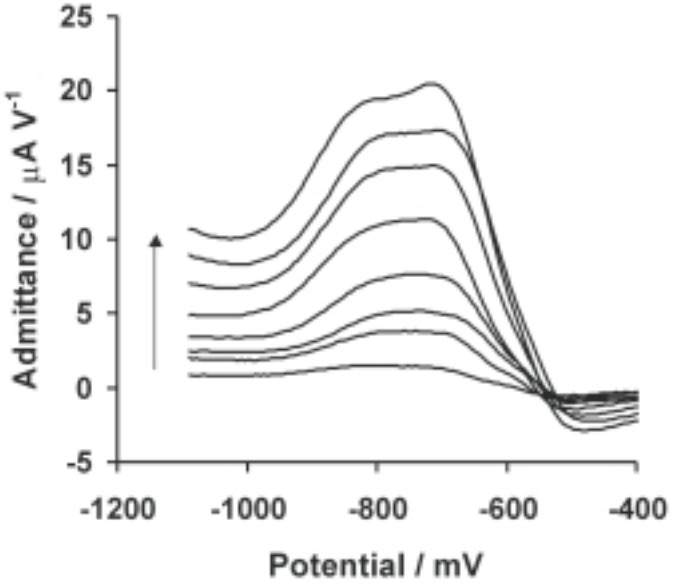

Figure 10. Changes in the admittance of a Pt microelectrode caused by an injection of glucose at concentrations 2×10^{-7}, 8×10^{-7}, 4×10^{-6}, 6×10^{-6}, 1×10^{-5}, 2.5×10^{-5}, 5×10^{-5} and 1×10^{-4} mol·dm^{-3} in 0.1 mol·dm^{-3} NaOH. The background admittance observed in 0.1 mol·dm^{-3} NaOH was subtracted. An arrow indicates increasing concentration of glucose.

After establishing the best determination conditions for sugars with the FFT SWV, this technique was used for monitoring the concentration of the carbohydrates during their separation in capillary electrophoresis. The electropherogram for an equimolar (0.1 mmol·dm^{-3}) mixture of eight sugars obtained with a Pt microelectrode is shown in Fig. 11. For comparison, an electropherogram for the same mixture of sugars, but with CV detection at an Au microelectrode is also shown in this figure. It is clear that the noise level during FFT SWV detection at a Pt microelectrode is considerably smaller than in the case of CV detection with Au electrode.

Introductory cyclic voltammetric studies of sugars were carried out to establish whether the use of microelectrodes and high scan rates make any essential difference in the studied processes. Similar research described in literature [8,10,25] was performed only at electrodes of standard (millimeter) size and typically at low scan rates. Analyses performed by us of the slopes (∂ logI/∂ log υ) for peaks observed at Pt and

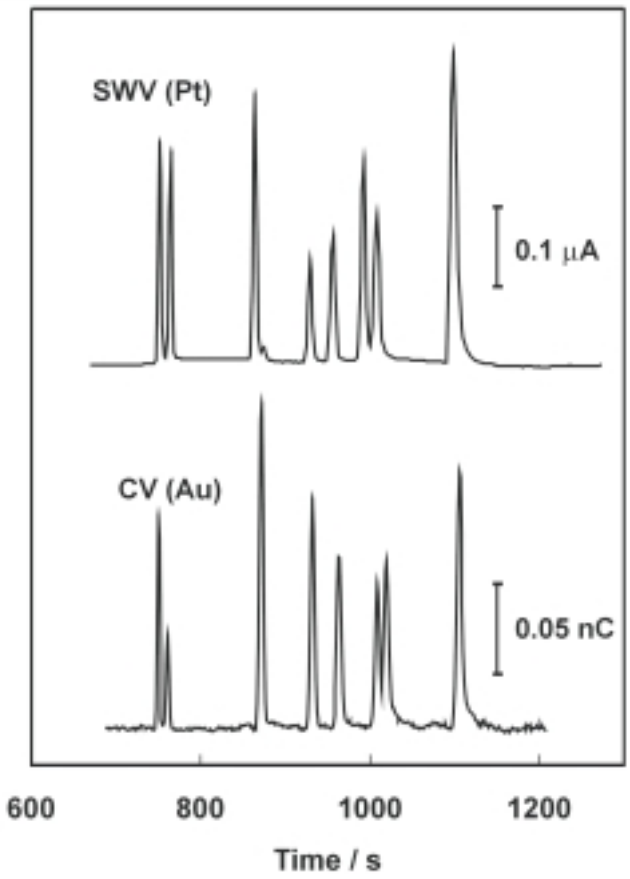

Figure 11. Comparison of electropherograms obtained for identical solutions with the FFT SWV detection at a Pt microelectrode (upper curve) and with the CV detection at an Au microelectrode (lower curve). The analyzed solution (0.5 nL) contained an equimolar (1×10^{-4} mol·dm^{-3}) mixture of eight sugars. CE conditions: fused silica capillary 25 μm I.D., 50 cm long, hydrodynamic injection, 0.1 mol·dm^{-3} NaOH as a running buffer, separation potentials – 12 kV. Consecutive peaks are for D-raffinose, sucrose, α-lactose, D-galactose, D-glucose, D-mannose, D-fructose and D-ribose.

Au microelectrodes give results similar to ones described in the literature, except for the anomalous high value for peak G_I (slope larger than 1.6). However, we do not intend to discuses mechanistic aspects of the process in this paper, but rather we will focus exclusively on the analytical aspects.

Up to now, most electrochemical detectors for sugars operate in various amperometric modes *i.e.* the response is measured at a constant potential (often, with two potential pulses added for cleaning the electrode surface). We, however, suggest, using scanned techniques such as cyclic voltammetry (CV) and square-wave voltammetry (FFT SWV). Amperometric detection provides the response in the form of a single number (value of current at a single potential). This approach has the advantage of simplicity, but when something goes wrong it is impossible to correct the data or even figure out what was wrong (whether the surface of the electrode changed

due to an increase of the surface roughness, or the electrode got contaminated, or a gas bubble was attached, or the potential shifted due to a change in a CE offset). From this point of view, scanning methods are much better than amperometric methods. First, the state of the electrode and the course of the detection experiment can be constantly monitored by observing the voltammograms (or square-wave voltammograms) recorded during the detection. Second, the electrode can be cleaned during each cycle by scanning it in a sufficiently wide range of potentials (approaching O_2 and H_2 evolution) or by applying two additional potential pulses with positive and negative potentials after each cycle, and the efficiency of the cleaning can be checked by examining the background current. Third, to achieve the most adequate determination conditions for given analytes, different potential and time/frequency settings can be used. Fourth, in CV and FFT SWV, the electrode response is measured not at one potential (like in amperometry), but over a wide range of potentials. The analytical signal is obtained by a numerical integration of the electrode response over some range of potentials. If the offset potential [20] in capillary electrophoresis changes during an amperometric detection, the measured signal may be lost, but in the scanning methods the signal only shifts into another potential region and it can be recovered by changing the integration range (that can be done at any time after the experiment using saved experimental data); usually there in no need to repeat the measurements. The change of the integration range can also be used, if necessary, to optimize the analytical response.

The use of microelectrodes allows us to carry the detection out in flowing solutions without the removal of dissolved oxygen and at higher scan rates that would be possible with electrodes of standard size.

Under CE conditions, the peak widths can be very narrow ($w_{1/2}$ from 2 to 5 s); therefore, low scan rates are not recommended. However, due to the nature of the electrode process (slow kinetics), the detection of carbohydrates in flowing solutions under CV conditions should not be carried out at scan rates higher than 2 $V \cdot s^{-1}$; that requirement causes a problem in the application of the CV technique to CE detection of sugars. Detection in the FFT SWV mode is, in this case, much more practical. The detection cycle (under optimum conditions) takes no longer than 0.6 s, consequently during each CE peak, the electrode is scanned four to eight times. The FFT SWV technique also offers a better S/N ratio than CV under capillary electrophoresis conditions.

Acknowledgments

This work was financially supported by the Polish State Committee for Scientific Research (KBN) (Grant No. 4 T09A 028 24 in 2003-2006).

REFERENCES

1. Yao S.J., Appleby A.J., Goreil A., Cash H.R. and Wolfson S.K., *Nature* (London), **224**, 921 (1965).
2. Reach G. and Wilson G.S., *Anal. Chem*., **64**, 381A (1992).
3. Beden B., Largeaud F., Kokoh K.B. and Lamy C., *Electrochim. Acta*, **41**, 701 (1996).
4. Luo P., Zhang F. and Baldwin R.P., *Anal. Chim. Acta*, **244**, 169 (1991).
5. Reim R.E. and Van Effen R.M., *Anal. Chem*., **58**, 3203 (1986).
6. Ueda T., Mitchell R., Kitamura F. and Nakamoto A., *J. Chromatogr.*, **592**, 229 (1992).
7. Kokoh K.B., Léger J.–M., Beden B. and Lamy C., *Electrochim. Acta*, **37**, 1333 (1992).
8. Governo A.T., Proença L., Parpot P., Lopes M.I.S. and Fonseca I.T.E., *Electrochim. Acta*, **49**, 1535 (2004).
9. Johnson D. and LaCourse W., *Anal. Chem*., **62**, 589 (1990).
10. Lei H.W., Wu B., Cha C.S. and Kita H., *J. Electroanal. Chem*., **382**, 103 (1995).
11. Vassilyew Yu.B., Khazowa O.A. and Nikolaeva N.N., *J. Electroanal. Chem*., **196**, 105, 127 (1985).
12. Larew L.A. and Johnson D.C., *J. Electroanal. Chem*., **262**, 167 (1989).
13. Makovos E.B. and Liu C.C., *Bioelectrochem. Bioenerg*., **15**, 157 (1986).
14. Lacourse W.R., Carbohydrate analysis by modern chromatography and electrophoresis, Ed. Ziad El Rassi, Elsevier 2002, Journal of Chromatography Library – volume 66, p. 905.
15. Buchberger W., *Fresenius J. Anal. Chem.*, **354**, 797 (1996).
16. Hughes S. and Johnson D.C., *Anal. Chim. Acta*, **132**, 11 (1981).
17. Kappes T. and Hauser P.C., *Electroanalysis*, **12, No. 3**, 165 (2000).
18. Wen J., Baranski A.S. and Cassidy R., *Anal. Chem*., **70**, 2504 (1998).
19. Baranski A.S. and Norouzi P., *Can. J. Chem*., **75**, 1736 (1997).
20. Magnuszewska J., Krogulec T. and Baranski A.S., *Chem. Anal. (Warsaw),* **45**, 189 (2000).
21. Gerhardt G.C., Cassidy R.M. and Baranski A.S., *Anal. Chem*., **72**, 908 (2000).
22. El Rassi Z., Carbohydrate analysis by modern chromatography and electrophoresis, Ed. Ziad El Rassi, Elsevier 2002, Journal of Chromatography Library – volume 66, p. 602.
23. Galus Z., Fundamentals of electrochemical analysis, Ellis Horwood, New York, London, Toronto, Sydney, Tokyo, Singapore and Polish Scientific Publishers PWN, Warsaw, 1994, pp. 145, 575.
24. Roberts R.E. and Johnson D.C., *Electroanalysis*, **6**, 269 (1994).
25. Baldwin R.P., Carbohydrate analysis by modern chromatography and electrophoresis, Ed. Ziad El Rassi, Elsevier 2002, Journal of Chromatography Library – volume 66, p. 947.
26. Essis Yei L.H., Beden B. and Lamy C., *J. Electroanal. Chem*., **246**, 349 (1988).
27. Morin S., Dumont H. and Conway B.E., *J. Electroanal. Chem*., **412**, 39 (1996).